Available online at www.sciencedirect.com

ScienceDirect

ARTICLE

Microstructure and Tribological Properties of WC-CeO$_2$/Ni-base Alloy Composite Coatings

He Long,   Tan Yefa,   Tan Hua,   Tu Yiqiang,   Zhang Zhongwei

PLA University of Science and Technology, Nanjing 210007, China

Abstract: The Ni-base alloy composite coatings synergistically reinforced by WC and CeO$_2$ particles were prepared on the surface of 7005 aluminum alloy by the plasma spray technique. The microstructures and the tribological properties of the composite coatings were researched. The results show that with the addition of CeO$_2$ particles, the microstructure of the composite coating is refined; meanwhile, the WC reinforcing particles change from round to irregular polygon and their decarburization are alleviated. The friction coefficients and the wear losses of the composite coatings are lower than those of the WC/Ni-base alloy composite coatings and the Ni-base alloy coatings at different PV values. When the PV values are smaller than 3.36 N·m/s, the maximum contact stress of the composite coating is lower than its elastic limit contact stress, the wear mechanisms of which are mainly micro-cutting wear and fatigue wear. As the PV values are bigger than 3.36 N·m/s, the maximum contact stress exceeds the elastic limit contact stress of the composite coating and the contact temperature sharply increases to 648 °C, obvious plastic deformation and desquamation traces appear on the worn surface and the wear mechanisms turn into multi-plastic deformation wear, abrasive wear and adhesive wear accompanied with oxidative wear.

Key words: composite coating; Ni-base alloy; tungsten carbide; cerium oxide; tribological property

---

Aluminum alloys have become the important materials to achieve lightweight of machinery due to their low density, high specific strength and good thermal conductivity, which are widely used in aerospace industry, motor industry, national defense industry etc.[1-3]. However, the low hardness and the poor wear resistance of aluminum alloys restrain their further applications in friction conditions. Owing to the excellent anti-wear, anti-corrosion and anti-oxidation properties, Ni-base alloys are effectively used as the surface strengthening coatings to meliorate the tribological properties of aluminum alloys frictional parts[4,5]. Nevertheless, the increasingly rigorous working conditions such as heavy load, high speed, high temperature and corrosive environment call for better anti-friction and anti-wear performance of Ni-base alloy coatings. Therefore, it is meaningful to further improve the tribological properties of Ni-base alloy strengthening coatings to extend service lives of aluminum alloy frictional parts.

Particle reinforced Ni-base alloy composite coatings exhibit both good toughness and wear resistance, which have been an important topic in the surface engineering field. Among all kinds of reinforcing particles, tungsten carbide (WC) is the most popular one used to reinforce Ni-base alloy coatings because of its extremely high hardness and excellent wear resistance[6,7]. Liu, et al [8] found that by incorporating WC particles, the wear resistance of Ni-base alloy coatings was improved, the maximum microhardness (12 500 MPa) and the minimum wear loss (0.06 g) of which were obtained with the WC particles volume fraction of 35%. Besides, some researches[9,10] revealed that the wear mechanism of Ni-base alloy coatings changed from a severe abrasive wear to a micro-cutting wear with the addition of WC particles, and the wear loss was obviously reduced. Rare earth cerium oxide (CeO$_2$) owns an excellent chemical activity owing to the special movement of 4f electronic-shell, and obvious effects are achieved on improving structure and the property of

---

coatings[11]. Cheng, et al[12] found that adding 0.5%~3.0% CeO_2 could prevent the bridge linking of reinforcing particles and refine the grains of coatings, and the microhardness of Ni-base alloy composite coatings was increased by 10% compared with that of the Ni-base alloy coating without CeO_2. Yuan[13] and Sharma[14] et al also testified that the wear resistance of Ni-base alloy coatings was improved by incorporating CeO_2 particles. It is obvious that either WC or CeO_2 particles are beneficial to improve the wear resistance of Ni-base alloy coatings. In case that these two kinds of particles are used simultaneously, whether the synergistic reinforcing effects between them can be formed will dramatically influence the tribological properties of coatings.

In order to study the synergistic reinforcing effects, WC and CeO_2 particles reinforced Ni-base alloy (WC-CeO_2/Ni-base alloy) composite coatings were prepared on the surface of 7005 aluminum alloy by plasma spray. The microstructure of the composite coating was researched and the tribological properties at different PV (*i.e.* P: Load ×V: Velocity) values were investigated to provide the references for the preparation and the application of multiphase particles synergistically reinforced composite coatings on aluminum alloy frictional parts.

1 Experiment

The sprayed materials consisted of Ni-base alloy powders, WC and CeO_2 particles, whose compositions are shown in Table 1. The chemical composition in wt% of Ni-base alloy powders with sizes ranging from 55 to 128 μm was 15.5Cr, 3.5B, 4.0Si, 15.0Fe, 3.0W, 0.8C and balance of Ni. WC-Co sintered particles (WC:Co=88:12) with sizes in the range of 37~74 μm were used as reinforcing particles. CeO_2 particles were 99.9% AR (Analytical Reagent) with average size of 20 μm.

7005 aluminum alloy was selected as substrates. Prior to spray, the substrates were treated by sanding, ultrasonic cleaning and sandblasting. The WC-CeO_2/Ni-base alloy composite coatings were prepared on the surface of substrates with the thickness of 200 μm by a DH-1080 plasma spray equipment. The technical parameters were current of 500 A, voltage of 50 V, argon flux of 70 L·min^{-1}, hydrogen flux of 10 L·min^{-1} and spray distance of 100 mm. The Ni-base alloy coatings and the WC/Ni-base alloy composite coatings were prepared as comparison. The sprayed specimens were ground by grinding wheel and W0.5 diamond abrasive paste, and then

Table 1   Composition of sprayed materials

Coating	Composition/wt%		
	Ni-base alloy	WC	CeO₂
Ni-base alloy coating	100	—	—
WC/Ni-base alloy composite coating	60	40	—
WC-CeO₂/Ni-base alloy composite coating	60	38	2

incised into test-pieces with the size of 12 mm×12 mm×6 mm.

Microstructures and worn surfaces were observed by a FEIQUANTA200 scanning electronic microscopy (SEM). Elemental composition was tested by an energy-dispersive X-ray analysis (EDAX) spectroscope attached to FEIQUANTA200. Metallographic images were obtained by a DMM330C optical microscope (OM). Phase composition was tested by a D-MAX/R X-ray diffractometer (XRD). Vickers microhardness was performed on a DHV-1000 microhardness tester. Bonding strength between the coating and the substrate was measured by a CMT(5105) electronic universal testing machine according to GB/T 8642-1988.

Tribological tests were carried out in an HT-500 ball-on-disc tribometer at room temperature (25 °C) with a sliding distance of 500 m. The upper specimen was a GCr15 ball with diameter of 4 mm, while the down one was a plate of specimens. The testing conditions were 3 N-0.28 m/s, 3 N-0.56 m/s, 12 N-0.28 m/s and 12 N-0.56 m/s (*i.e.* PV values of 0.84 N·m/s, 1.68 N·m/s, 3.36 N·m/s and 6.72 N·m/s). Friction coefficients were tested automatically by the software attached to HT-500 and wear losses were measured by a TG328B balance with precision of 0.1 mg.

2 Results and Discussion

2.1 Microstructure

The morphologies of the coatings are shown in Fig.1. It shows that the surface of Ni-base alloy coating is flat but with some pores (Fig.1a), and on the surface of the WC/Ni-base alloy composite coating there exist a few pores, cracks and plenty of round gray areas (marked by A) as shown in Fig.1b. According to the EDAX spectrum of area A (Fig.2a), the atom ratio of W:C is almost 1:1 indicating that is the WC reinforcing phase. The WC-CeO_2/Ni-base alloy composite coating is flat and dense without obvious pores and microcracks, in which the WC reinforcing phase takes on irregular polygon (Fig.1c). Moreover, the composite coating integrates tightly with the aluminum alloy substrate. There are no cracks and pones appeared at interface (Fig.1d), and the bonding strength between them reaches 31.6 MPa. Besides, the chemical elements of dark area marked by B are Ni, Fe, Cr and Si, and the mass fraction of Ce is 0.46% (Fig.2b), which indicates that CeO_2 particles melted well in Ni-base alloy matrix. From Fig.2c, it can be inferred that element Ce is enriched (1.68%) at the interface (marked by C) between WC and Ni-base alloy. Owing to the high temperature of plasma arc, CeO_2 particles can be decomposed to generate Ce atoms that own good chemical activity and are easy to be absorbed on the surface of molten WC particles to improve their fluidity[15]; meanwhile, element diffusion and mass transfer capabilities among WC particles and Ni-base alloy are enhanced. Therefore, the WC particles change from round to irregular polygon, which extends the bonding interface and improves the bonding strength among WC particles and Ni-base alloy.

Fig.1   Surface morphologies of Ni-base alloy coating (a), WC/Ni-base alloy composite coating (b), WC-CeO₂/Ni-base alloy composite coating (c), and cross section image of C-CeO₂/Ni-base alloy composite coating (d)
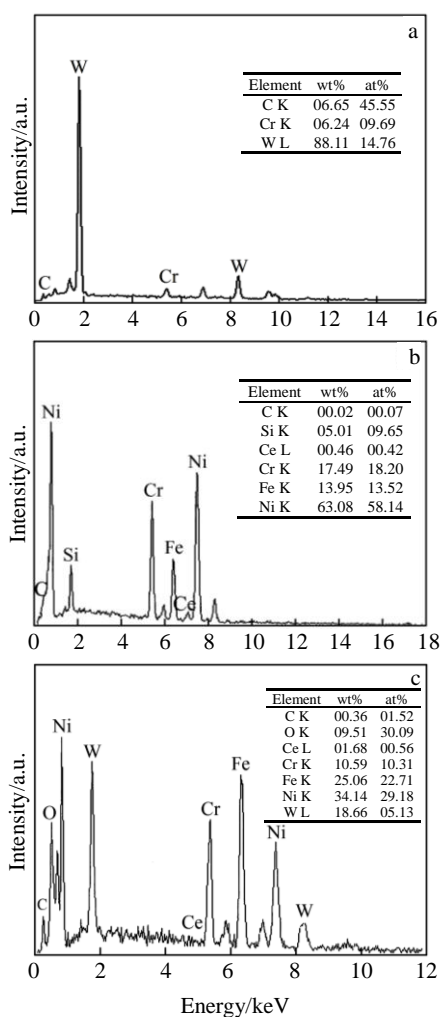
Fig.2   EDAX spectra of area A (a), area B (b), and area C (c) in Fig.1

Fig.3 is the XRD patterns of the coatings. It reveals that the phase composition of the WC-CeO₂/Ni-base alloy composite coating is γ-Ni, $Cr_{23}C_6$, CrB, $FeNi_3$, WC, W_2C and Co_3W_3C. The existence of W_2C and Co_3W_3C phases indicates that decarburization and decomposition of WC particles occurs by the reactions as follow[16]:

$$2WC \rightarrow W_2C + C \tag{1}$$
$$4Co + 4WC + O_2 \rightarrow 2Co_2W_4C + 2CO \tag{2}$$
$$3Co + 3WC + O_2 \rightarrow Co_3W_3C + 2CO \tag{3}$$
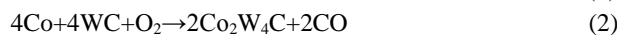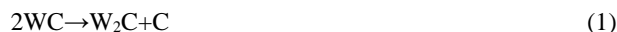
Although the W_2C phase is of high hardness, the brittleness of the composite coating may be increased, and then it results in brittle fracture and severe wear. As shown in Fig.3, the diffraction peak area and intensity of W_2C and Co_3W_3C in WC-CeO₂/Ni-base alloy composite coating are smaller than those in the WC/Ni-base alloy composite coating, which indicates that incorporating CeO₂ particles is helpful to alleviate decarburization and decomposition of WC particles, and more reinforcing particles can be retained in WC-CeO₂/Ni-base alloy composite coating. This is because the CeO₂ particles of high melting point around WC reinforcing phase can absorb a mass of heat to prevent severe decomposition of WC particles.

The major diffraction peak at $2\theta=44.12°$ of WC-CeO₂/Ni-base alloy composite coating is wider than that of the WC/Ni-base alloy composite coating. According to the Scherrer formula [17]:

$$d = \frac{K\lambda}{\beta \cos\theta} \tag{4}$$

where, d is the grain size, K is constant, λ is the wavelength of X-ray, β is the full width at half maximum (FWHM), and θ is the diffraction angle.

It is inferred that the grain size (d) of the major phase decreases with the increase of FWHM (β), so the microstructure of the composite coating is refined as shown in Fig.4. The Ce atoms with big radius and strong electronegativity can aggregate at the grain boundary, so the grain boundary migration and grain growth are blocked. In addition, Ce atoms are beneficial to reduce interface energy and critical
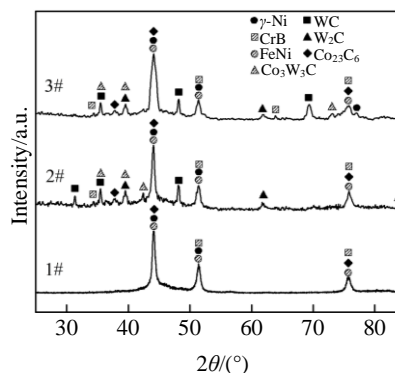
Fig.3   XRD patterns of Ni-base alloy coating (1#), WC/Ni-base alloy composite coating (2#) and WC-CeO₂/Ni-base alloy composite coating (3#)
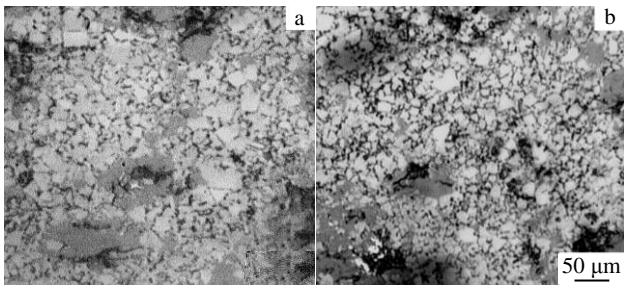
Fig.4 Metallographic images of WC/Ni-base alloy composite coating (a) and WC-CeO2/Ni-base alloy composite coating (b)

nucleation energy[18], so the nucleation ratio of the composite coating is increased resulting in a grain refinement effect. The microhardness of the WC-CeO2/Ni-base alloy composite coating is HV$_{0.5}$ 7925 MPa, which is 5.5% and 33.6% higher than that of the WC/Ni-base alloy composite coating and the Ni-base alloy coating, respectively. It is attributed to the synergistic effects of dispersion strengthening caused by WC reinforcing particles and grain refinement of Ni-base alloy caused by CeO2 particles.

2.2 Tribological behaviour

The tribological results of WC-CeO2/Ni-base alloy composite coatings at different PV values are shown in Fig.5. It exhibits that the friction coefficients of the composite coatings increase from 0.29 to 0.42 as PV values increase, which are lower than those of the WC/Ni-base alloy composite coatings (0.33~0.48) and the Ni-base alloy coatings (0.35~0.52) (Fig.5a). As shown in Fig.5b, the wear losses of all three kinds of coatings take on increasing trends, and the WC-CeO2/Ni-base alloy composite coating possesses the lowest value, especially at 6.72 N·m/s, its wear loss is sharply reduced by 29.4% and 47.4% compared with those of other two kinds of coatings.

The improvement on wear resistance of the composite coating is mainly attributed to three reasons. Firstly, the uniformly distributed WC reinforcing particles act as anti-wear pivots to prevent Ni-base alloy matrix from severe abrasion caused by GCr15 steel ball counterpart. Secondary, with the addition of CeO2 particles, the grains of the composite coating are refined. According to the Hall-Petch formula as follow[19]:

$$\sigma_1 = \sigma_0 + kd_1^{-0.5} \tag{5}$$

where, σ_1 represents the strength of the composite coating, σ_0 and k are the constants of grains, and d_1 is the grain diameter.

It is obvious that the strength of the composite coating (σ_1) increases as grain diameter (d_1) decreases, which improves the plastic deformation resistance of the composite coating in frictional process, and enhances its wear resistance[20].

Thirdly, the fluidity and filling ability of molten particles are boosted up by adding rare earth, and Ce atoms are prone to
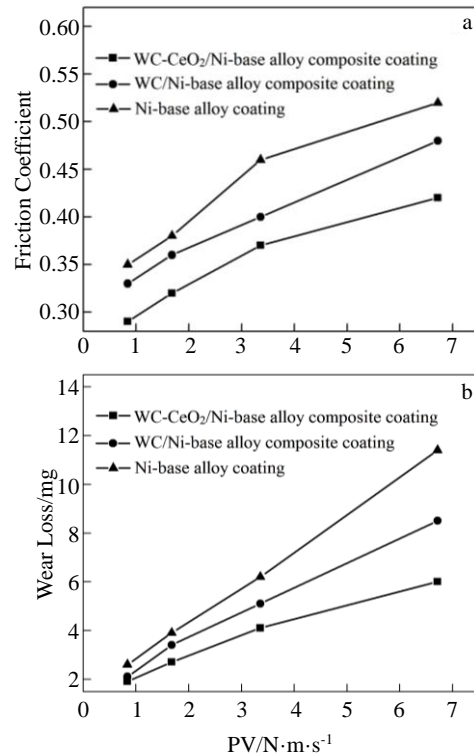
Fig.5 Friction coefficient (a) and wear loss (b) of WC-CeO2/Ni-based alloy composite coatings at different PV values

react with elements O and N in residue air that is helpful to reduce the inclusions and pores in the composite coating[21]. As a result, the microstructure of the composite coating is improved to increase its fracture toughness, which can restrain the crack initiation and propagation, and then reduce the worn off of WC particles. Therefore, the grain refinement and the microstructure purification of the composite coating caused by element Ce improves the bonding strength between WC particles and Ni-base alloy, together with the synergistic effects of WC anti-wear reinforcing phase that make the WC-CeO2/Ni-base alloy composite coating possess better tribological properties than the WC/Ni-base alloy composite coating and the Ni-base alloy coating.

2.3 Wear mechanisms

Load and speed are the important external factors that affect the friction and wear properties of WC-CeO2/Ni-base alloy composite coating by changing its surface stress field and temperature field. In frictional process, PV value can token the effects on tribological behavior and mechanisms of the composite coating caused by load and speed simultaneously. Actually, the stress state of worn surface is mainly determined by load. Therefore, the Hertz formula of rigid sphere and elastic half plane contact under normal load can be used to calculate the maximum contact stress on contact area, *i.e.*[22]:

$$p_0 = \left[\frac{6P}{\pi^3 R^2} \left(\frac{E}{1-v^2} \right)^2 \right]^{1/3} \tag{6}$$

where, p_0 is the maximum contact stress (MPa), P is the normal load (N), E is the elastic modulus of the composite coating (GPa), v is the poisson's ratio of the composite coating, and R is the comprehensive curvature radius (m), *i.e.* $R^{-1}=R_1^{-1}+R_2^{-1}$, R_1 and R_2 are the curvature radius of the frictional pairs.

Elastic limit contact stress of the composite coating characterizes its maximum permissible contact stress when plastic deformation happens. If the maximum contact stress is higher than the elastic limit contact stress, yield flow and plastic deformation of the composite coating will be generated, which may result in severe wear. The theoretical formula of the elastic limit contact stress (p_y) is as follows [23]:

$$p_y = \frac{\frac{1}{2.8 \times 1.854} H_v \cdot 2g \sin\left(\frac{\alpha}{2}\right)}{\left[\frac{(1-2v)^2}{3} + \frac{\mu\pi(1-2v)(2-v)}{4} + \frac{\mu^2\pi^2(16-4v+7v^2)}{64}\right]^{1/2}} \quad (7)$$

where, H_v is the microhardness of the composite coating (kg/mm^2), α is the taper indenter angle with 136°, and μ is the friction coefficient under different PV values.

The maximum contact stress (p_0) and the elastic limit contact stress (p_y) of the composite coating at different PV values are listed in Table 2.

In dry friction conditions, plenty of frictional heat will be generated on worn surface under the simultaneous actions of load and speed, which results in the increase of contact temperature in local contact area, and furthermore affects the wear mechanisms. The contact temperature can be calculated by the formula as follows[24]:

$$T_c = T_0 + A\sqrt{\frac{2a}{V_r}} \cdot \frac{\gamma\mu\sigma_m V_r}{\sqrt{K\rho C}} \quad (8)$$

where, T_c is the contact temperature (°C), T_0 is the bulk temperature (°C), A is coefficient and for circular contact is 1.11, a is the contact radius (m), V_r is the sliding velocity (m/s), γ is the heat distribution coefficient, μ is the friction coefficient, σ_m is the average contact stress (MPa), K is the thermal conductivity (W/m·°C), ρ is the density (kg/m^3), and C is the specific heat capacity (kJ/kg·°C).

The heat distribution coefficient (γ) in Eq. (8) can be expressed by Eq. (9) as follow:

$$\gamma = \frac{0.627K\left(a\rho V_r C / K\right)^{1/2}}{K_1 + 0.627K\left(a\rho V_r C / K\right)^{1/2}} \quad (9)$$

where, K_1 is the thermal conductivity of GCr15 steel ball counterpart (W/m·°C).

Table 2   Maximum contact stress and elastic limit contact stress at different PV values

PV value/N·m·s^{-1}	0.84	1.68	3.36	6.72
Maximum contact stress/MPa	2927	2927	4646	4646
Elastic limit contact stress/MPa	3923	3546	3292	2667

Besides, the contact radius (a) in Eq. (8) can be obtained by the formula as follows:

$$a = \left[\frac{3PR}{4}\left(\frac{1-v^2}{E}\right)\right]^{1/3} \quad (10)$$

Table 3 lists the contact temperature of the worn surface at different PV values.

The typical worn surface morphologies of the composite coatings at different PV values are shown in Fig.6. It is found that there are only a few shallow and discontinuous scratches appearing on the worn surface at the PV value of 0.84 N·m/s (Fig.6a). Because the maximum contact stress of the worn surface (2927 MPa) is smaller than its elastic limit contact stress (3923 MPa), and the contact temperature is only 123 °C, so no plastic deformation occurs in frictional process. The composite coating is in a slight wear condition and its wear mechanism is mainly micro-cutting wear.

As the PV value increases to 1.68 N·m/s, deep scratches, obvious microcracks and fatigue desquamation turn up on the worn surface as shown in Fig.6b. As a result of speed increasing, the contact temperature reaches 171 °C, which leads to the decrease in hardness of coating materials and results in deep scratches by the friction of GCr15 counterpart. Besides, the action frequency of GCr15 counterpart on the worn surface also increases, so the microcracks are prone to be formed in maximum shear stress area near drawbacks of the composite coating under repeating extrusion and abrasion[25], and then propagate to surface and result in the partial fatigue desquama-

Table 3   Contact temperature at different PV values

PV value/N·m·s^{-1}	0.84	1.68	3.36	6.72
Contact temperature/°C	123	171	309	648
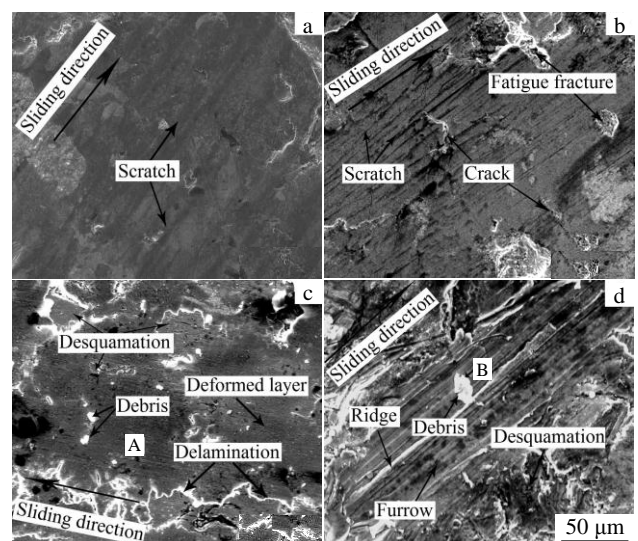
Fig.6   Typical worn surfaces morphologies of WC-CeO$_2$/Ni-base alloy composite coatings at different PV values: (a) 0.84 N·m/s, (b) 1.68 N·m/s, (c) 3.36 N·m/s, and (d) 6.72 N·m/s

tion of the composite coating. Therefore, the composite coating suffers from micro-cutting wear and fatigue wear at 1.68 N·m/s.

When the PV value is 3.36 N·m/s, obvious plastic deformation, delamination and desquamation as well as fine wear debris are formed on the worn surface (Fig.6c). In this friction condition, the maximum contact stress of the worn surface is 4646 MPa, which is much higher than its elastic limit contact stress of 3292 MPa, so the plastic flow and deformation of coating materials occurs. At the same time, the mechanical properties such as hardness and strength of the composite coating are further decreased as the contact temperature increases to 309 °C, which aggravates the plastic deformation extent and results in mechanical mixed layer (MML) [26]. The MML experiences working hardening as a result of repeating plastic deformation, and its brittleness increases that makes it prone to be desquamated under the friction of GCr15 counterpart. The EDAX spectrum of the deformed area marked by A is depicted in Fig.7a. It reveals that the content of element O on the worn surface is 44.25%, which indicates that oxidation reactions may happen in frictional process as follows:

$$2Ni+O_2 \rightarrow 2NiO \tag{11}$$
$$4Fe+3O_2 \rightarrow 2Fe_2O_3 \tag{12}$$
$$4Cr+3O_2 \rightarrow 2Cr_2O_3 \tag{13}$$

Due to the high contact temperature, chemical activity of the worn surface improves, which makes it easy to react with element O in air. Therefore, the wear mechanisms of the composite coating are mainly multi-plastic deformation wear and oxidative wear at the PV value of 3.36 N·m/s.
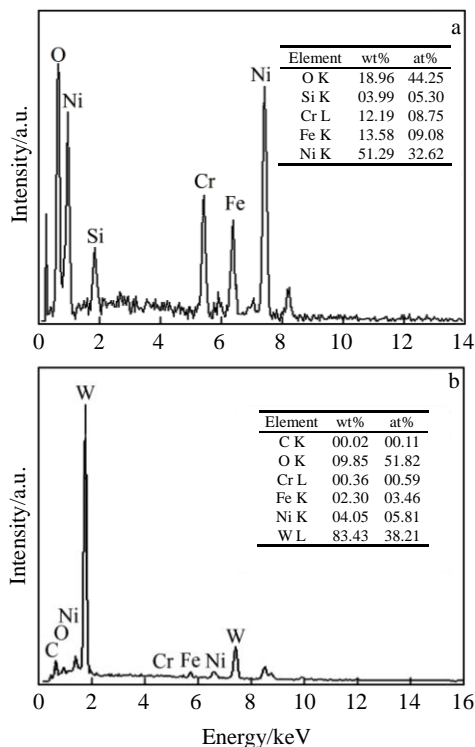
At the high PV value of 6.72 N·m/s, the composite coating suffers from much more severe wear. There are wide and deep furrows, obvious ridge and piece wear debris as well as adhesive desquamation traces appearing on the worn surface as shown in Fig.6d. Both load and speed are at the maximum value in this friction condition, and the contact temperature sharply increases to 648 °C, which is 2.1 times as high as that at 3.36 N·m/s. The weakening effects on hardness and strength of coating materials are further aggravated, so the worn surface is extruded and cut to generate furrows and ridges under high contact stress. Besides, elements diffusion capacity between frictional pairs also improves with the increase of temperature. Welding-on between the worn surface and the GCr15 counterpart happens, but by the continuous action of shearing stress, the worn surface is avulsed to form the adhesive desquamation traces[27]. According to the EDAX spectrum of the wear debris marked by B (Fig.7b), the main chemical elements are W and O, which indicates that it is the oxidized WC reinforcing phase. This is because that some WC particles own low bonding strength with the Ni-base alloy matrix, which are easy to be worn off and oxidized in frictional process, and furthermore, act as abrasive to deteriorate the abrasive wear. It is obvious that the wear mechanisms of the composite coating change into severe abrasive wear and adhesive wear accompanied with oxidative wear in high PV value (6.72 N·m/s) frictional condition.

3　Conclusions

1) With the addition of CeO_2 particles, the microstructure of WC-CeO_2/Ni-base alloy composite coating is refined, and the WC reinforcing phase change from round to irregular polygon and its decarburization and decomposition are alleviated. The microhardness ($HV_{0.5}$) of WC-CeO_2/Ni-base alloy composite coating is 7925 MPa, which is 5.5% and 33.6% higher than that of the WC/Ni-base alloy composite coating and the Ni-base alloy coating, respectively.

2) With the increase of PV values, the friction coefficients of WC-CeO_2/Ni-base alloy composite coatings vary in the range of 0.29~0.42, which are smaller than those of the WC/Ni-base alloy composite coatings (0.33~0.48) and the Ni-base alloy coating (0.35~0.52). The wear losses of the composite coatings change from 1.9 to 6.0 mg, and the average value is decreased by 23% and 39% compared with that of the WC/Ni-base alloy composite coatings and the Ni-base alloy coatings, respectively.

3) When the PV values are smaller than 1.68 N·m/s, the composite coating bears low contact stress compared with its elastic limit contact stress, and its wear mechanisms are mainly micro-cutting wear and fatigue wear. As the PV values increase to 3.36 N·m/s, the composite coating suffers from multi-plastic deformation wear and oxidative wear because of the high contact stress of 4646 MPa. At high PV value of 6.72 N·m/s, the contact stress and the contact temperature simultaneously reach the maximum value of 4646 MPa and 648 °C, respectively. The

Element	wt%	at%
O K	18.96	44.25
Si K	03.99	05.30
Cr L	12.19	08.75
Fe K	13.58	09.08
Ni K	51.29	32.62

Element	wt%	at%
C K	00.02	00.11
O K	09.85	51.82
Cr L	00.36	00.59
Fe K	02.30	03.46
Ni K	04.05	05.81
W L	83.43	38.21

Fig.7　EDAX spectra of area A (a) and area B (b) in Fig.6

composite coating is in a severe wear condition and its mechanisms change into abrasive wear, adhesive wear and oxidative wear.

References

1　Chen Zhiguo, Yang Wenling, Wang Shiyong *et al. Rare Metal Materials and Engineering*[J], 2010, 39(8): 1499 (in Chinese)

2　Bolelli G, Lusvarghi L, Barletta M. *Wear*[J], 2009, 267: 944

3　Xiao Bing, Kang Feng, Hu Chuankai *et al. Ordnance Material Science and Engineering*[J], 2011, 43(1): 94 (in Chinese)

4　Serres N, Hlawka F, Costil S. *Journal of Thermal Spray Technology*[J], 2010, 12: 49

5　He L, Tan Y F, Cai B *et al. Advanced Materials Research*[J], 2012, 538-541: 207

6　Chivavibul P, Watanabe M, Kuroda S *et al. Journal of Thermal Spray Technology*[J], 2011, 20(5): 1098

7　Li Yefei, Gao Yimin, Wang Bihui *et al. Rare Metal Materials and Engineering*[J], 2010, 39(4): 715 (in Chinese)

8　Liu Xingbao, Yao Guanxin, Gao Dong *et al. Materials for Mechanical Engineering*[J], 2011, 35(5): 62 (in Chinese)

9　Yao Shunhui. *Tribology*[J], 2009, 29(3): 193

10　Jha A K, Gachake A, Prasad B K *et al. Journal of Materials Engineering and Performance*[J], 2002, 11(1): 37

11　Shi Peng, Luo Lizhu, Huang Li *et al. Rare Metal Materials and Engineering*[J], 2010, 39(S1): 391 (in Chinese)

12　Cheng Xiyun, He Keshan, He Jun. *Tribology*[J], 2010, 30(3): 250

13　Yuan Jinping, Zhang Ping, Liang Zhijie *et al. Rare Metal Materials and Engineering*[J], 2008, 37(1): 147 (in Chinese)

14　Sharma S. *Journal of Thermal Spray Technology*[J], 2012, 21(1): 49

15　Wang Hongxing, Li Yingguang, Chu Chenglin. *Rare Metal Materials and Engineering*[J], 2011, 40(2): 316 (in Chinese)

16　Bao Junfeng, Hou Yubai. *Thermal Spray Technology*[J], 2010, 2(2): 45

17　Lemine O M. *Superlattices and Microstructures*[J], 2009, 45: 576

18　Yan Yonggen, Li Mingxi, Zhang Shihong *et al. Journal of the Chinese Rare Earth Society*[J], 2007, 25(5): 620 (in Chinese)

19　Miura S, Ono N, Nishimura Y. *Journal of The Society of Material Science, Japan*[J], 2009, 58(10): 865

20　Zhou Yuebo, Zhang Haijun. *Rare Metal Materials and Engineering*[J], 2008, 37(3): 448 (in Chinese)

21　Liu Guanghua. *Rare Earth Materials and Application Technology*[M]. Beijing: Chemical Industry Press, 2005, 29 (in Chinese)

22　Popov V L. *Contact Mechanics and Friction Physical Principles and Applications*[M]. Beijing: Tsinghua University Press, 2011 (in Chinese)

23　Bhushan B. *Introduction to Tribology*[M]. Beijing: China Machine Press, 2006 (in Chinese)

24　Liu Zuomin. *Tribology Theory and Design*[M]. Wuhan: Wuhan University of Science and Technology Press, 2009 (in Chinese)

25　Tan Y F, Cai B, He L *et al. Advanced Materials Research*[J], 2012, 415-417: 2191

26　Venkataraman B, Sundararajan G. *Wear*[J], 2000, 245: 22

27　Liu S L, Zheng X P, Geng G Q. *Materials and Design*[J], 2010, 31: 913

WC-CeO₂/镍基合金复合涂层的微观结构与摩擦学性能

何　龙，谭业发，谭　华，屠义强，张中威

(解放军理工大学，江苏 南京 210007)

摘　要： 运用等离子喷涂技术在 7005 铝合金表面制备了 WC 和 CeO₂ 颗粒协同增强镍基合金复合涂层，研究了该复合涂层的微观结构和摩擦学性能。结果表明：加入 CeO₂ 颗粒细化了复合涂层的显微组织，使 WC 增强颗粒从圆形变为不规则多边形，并降低了其脱碳分解程度。不同 PV 值摩擦条件下，WC-CeO₂/镍基合金复合涂层的摩擦系数和磨损失重均低于 WC/镍基合金复合涂层和镍基合金涂层。PV 值小于 3.36 N·m/s 时，复合涂层磨损表面的最大接触应力低于其弹性极限接触应力，主要发生微观切削磨损和疲劳磨损；PV 值大于 3.36 N·m/s 后，磨损表面的最大接触应力超过其弹性极限接触应力，接触温度也急剧上升至 648 ℃，磨损表面出现明显的塑性变形和脱落，其磨损机制变为多次塑变磨损、磨粒磨损和粘着磨损，并伴有氧化磨损。

关键词： 复合涂层；镍基合金；碳化钨；氧化铈；摩擦磨损

作者简介：何　龙，男，1986 年生，博士生，解放军理工大学野战工程学院，江苏 南京 210007，E-mail: helong19861009@163.com